Microwave Review
December 2024, Vol. 30, No. 2, pp. 99-123
DOI: 10.18485/mtts_mr.2024.30.2.13

Microwave and mm-Wave Band-Wise Microstrip Line-to-Waveguide Transitions: A Review

Atul Varshney

Abstract –**This study presents a detailed comparative review of microwave and mm-wave band-wise microstrip-to-waveguide transitions for MMIC/MIC interconnect transmitter/receiver front-end connections in microwave, mm-wave, and sub-mm-wave applications. All microwave band microstrip-to-rectangular waveguide transitions from 4 GHz (C-band) to 325 GHz (Y-band) have been reviewed and compared in terms of their performance parameters like return loss (RL), insertion loss (IL), and their relative or fractional bandwidth. This survey also highlights the requirement for appropriate substrates for distinct operating bands in PCB fabrication, which include extracted dielectric permittivity, loss tangents, and necessary thicknesses. The literature also strongly talks about the suitable rectangular waveguide needed for a particular waveguide with its dimensional information. The comparison also talks about the type of transitions (inline or vertical), and the and the coupling methodology used for transitions merits and demerits along with their applications. The outcome of this detailed review is that it describes all the methodological steps involved, along with mathematical expressions and their performance parameters, for new researchers and scientists in this particular area.**

Keywords – **Coaxial cable, Interconnects, Launcher, Microstrip antenna, Microstrip line, Microwave bands, Rectangular waveguide, Transition.**

I. INTRODUCTION

The significant number of RF and microwave activities in the sub-millimeter and mm-wave frequency ranges in areas such as communications, imaging, automotive radar, and tracking radar has raised the demand for systems and components in this range. Waveguide-based components are employed as a power feed network to fulfill the high-power requirements in these frequency ranges. Waveguides frequently replace coaxial cables as the primary transmission line in mm-wave due to their ease of manufacture and reduced loss. Planar-technology components, such as monolithic microwave integrated circuits (MMICs), are essential. As a result, for these purposes, a low insertion loss and broadband transition between both the microstrip line and waveguide are critical. Furthermore, due to a scarcity of connections at millimetres and terahertz frequencies, most measurement equipment is waveguide-based, necessitating the switch.

There are several types of microstrip-to-waveguide transitions, depending on their applications; Such designs include those based on ridged waveguides, antipodal fin lines, coupling probes, dipole antennas, substrate-integrated waveguides (SIW), iris coupling, among others. To communicate a signal, transmission lines transport energy from input to output ports. Waveguides, coaxial lines, planar transmission lines, microstrip lines, coplanar waveguide lines, and slot lines are some examples. For the effective deployment of microwave systems, engineers use a variety of transmission line types, coupling the electromagnetic wave from one type to another via appropriate transitions. For any of these transitions, transmission and reflection losses must be low.

The main objective of this paper is to present a user-friendly microwave band-wise survey from C-band (4 GHz–8 GHz) to Sub-mm Wave Y-band (220 GHz–325 GHz) in terms of performance parameters (return loss, insertion loss, and bandwidth) with detailed coupling methodology used and main features of the transitions to reduce tedious studies. Also, another aim of this article is to address the different confusing definitions of relative bandwidth, fractional bandwidth, and absolute bandwidth, return loss, insertion loss, reflection coefficients, and transmission coefficients.

Article history: Received March 10, 2024; Accepted May 15, 2024

Atul Varshney is with the Faculty of Electronic and Communication Engineering Department, FET, Gurukula Kangri (Deemed to be University), Haridwar, Uttarakhand, India, E-mail: atulgkvright@gmail.com

II. LITERATURE REVIEW

To communicate a signal, transmission lines transport energy from input to output ports. Waveguides, coaxial lines, planar transmission lines, microstrip lines, coplanar waveguide lines, and slot lines are some examples. Engineers utilize various types of transmission lines to effectively deploy microwave systems, coupling the electromagnetic wave from one type to another through appropriate transitions. For any of these transitions, transmission and reflection losses must be low. This blog article addresses the hybrid microstrip to waveguide transition, one of several types of transitions that are commonly used in microwave circuit design:

(i) Transition from waveguide to planar
(ii) Transition from coaxial to waveguide
(iii) Transition from Rectangular Waveguide to elliptical waveguides.

Waveguides are a good choice for high-power, low-loss transmission, but they are also big and costly. Microstrip lines, for example, have found popularity in the microwave field because of their small dimensions and ease of integration with transistors and diodes to produce microwave-integrated circuits (MICs). For these reasons, a transition from a waveguide to a planar transmission line is appropriate for a wide range of microwave systems.

Transitions from a waveguide to a planar transmission line may be roughly categorized into three types: in-line (0˚) transitions, aperture coupling transitions, and transverse transitions (90˚). In inline, transition takes place in the direction of propagation of the waveguide [1, 2, 4, 10, 11, 14,

28, 30, and 31]. In aperture-coupled transitions, energy is coupled to the planar transmission line via the aperture, which can be located on the waveguide's end wall or broad wall [8], whereas in transverse transitions, the probe is transverse to the waveguide's propagation direction [5, 13, 20 and 23]. Consequently, these transitions sometimes refer to these transitions as 'broadside' and 'narrow side' wall transitions. In comparison to inline transitions, these take up significantly more space and volume. Despite this, these transitions have a lower return loss and a wider bandwidth. The intricacy of these structures is their sole downside [3, 6-9, 12, 14-17, 21, 22, 24-27, and 29]. A microstrip antenna is used as an energy coupling element in the rectangular waveguide. As a result, the microstrip antenna serves as an energy launcher within the waveguide and is an essential subset of the transitions. Most widely, Quasi-Ygai Uda, bow-tie launcher, radial probe coupled, semi-circular loop coupled, dipole, rectangular, circular, patch, monopole, slot, etc. antennas are used as microstrip launchers in the rectangular waveguide [5, 18, 20, 21, 23, 26, 46]. The slot coupling, magnetic coupling, and aperture coupling are generally used coupling methods for MS-to-WG transitions [5, 13, 21, 34]. The most widely transmitted mode of the waveguide is transverse electric mode (TE_{10}) [25]. Air-filled, dielectric-filled, tapered ridges, and multi-stepped ridge rectangular waveguides (RWG) are utilized for energy output components in the transitions [13, 20, 40, and 44]. Multi-step probe coupling is the most commonly used coupling technique [25, 52]. Complementary split ring resonator (CSRR) patches and comb-like structures were used to broaden the bandwidth and enhance the coupling efficiency [21, 41]. An embedded wafer-level ball grid array (eWLB) and electronic band gap (EBG) patches are used to reduce parallel mode and radiation losses [50, 51]. Detailed comparative studies of MS-to-RWG transitions for microwave, mm-wave and RADAR applications have been discussed in reference [53]. The drawback of that survey is that a lengthy table and mixed band details are presented. No transition had been designed in L-band or S-band. That's why a new study for a band always needs to separate information extraction from the table by reworking that. From the researcher's point of view, a more user-friendly microwave and mm-wave band-wise survey from C-band to Y-band has been presented in this article, with a greater collection of literature for microwave, mm-wave, and sub-mm-wave applications.

III. Transition Design and Methodology

To design an MS-to-RWG transition, first choose the applications, and as per the application, select the desired microwave band and suitable substrate waveguide type (WR-XX), then evaluate all the related waveguide secondary parameters using formulas given in references [37, 53]. Then evaluate the microstrip line secondary parameters using the chosen substrate dielectric constants, thickness, and loss tangent for the operating frequency band using formulas given in references [36, 53]. A slot is placed from the quarter wavelength ($\frac{\lambda_g}{4}$) apart from the back-short distance of the waveguide in case of transverse, transitions as represented in Figure 1(a) [25, 52]. Sometimes transition designs eliminate

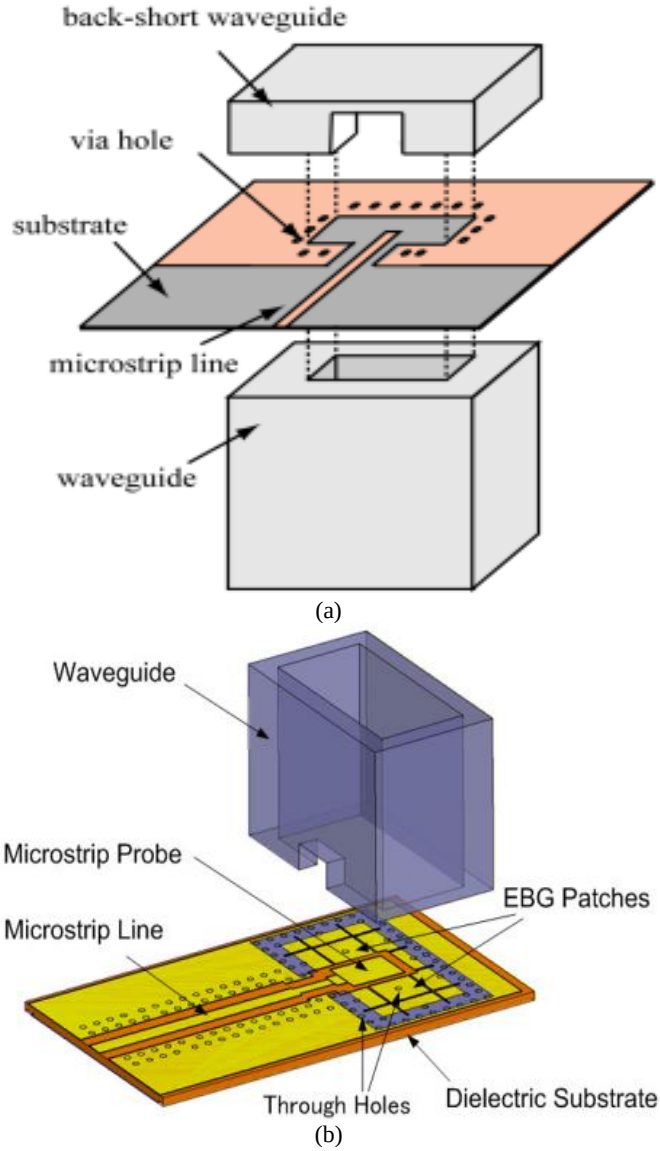

Fig. 1. Transverse Transition: (a) With Back-Short MS-to-WG Transverse E-Plane Transition [54], (b) back short-less MS-to-WG Transverse E-Plane Transition with EBG structure [39]

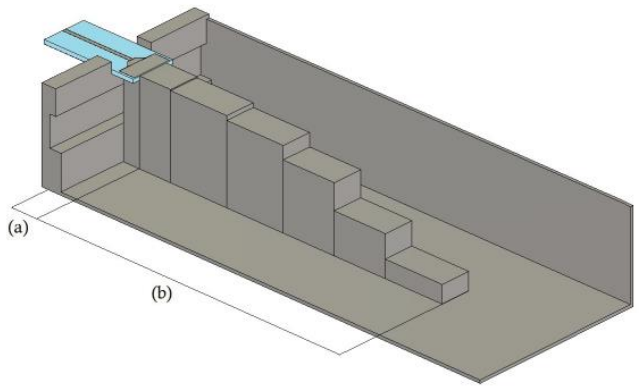

Fig. 2. (a) Inline transition (launcher), (b) matching impedance structures [31]

the need for waveguide back-shorting and reduce the need for hardware and, therefore cost. Simply put, we can say that the microstrip is placed transverse to the direction of propagation at the bottom end of the rectangular waveguide, and the output is taken from the far end of the waveguide, as represented in Figure 1(b) [39]. Similarly, in the case of inline transitions, no need for waveguide back-short as depicted in Figure 2 [1, 2, 4, 10, 11, 14, 28, 30, and 31]. The planar microstrip line has a low impedance (50 Ω) as compared to air-filled, dielectric, or ridge rectangular waveguides (400 Ω-500 Ω). Thus, impedance matching is one of the biggest challenges for the design of MS-to-WG transitions. Yet another challenge of this transition design is to match the modes of wave propagation since both transmission lines have different modes (quasi-TEM mode in the MS line, whereas transverse electric, TE_{10} dominant mode in RWG). For impedance matching purposes, many of the quarter-wave, multi-stepped, and Chebyshev's impedance matching transformer techniques are used. The mode matching among the two transmission lines has been achieved by a change in the slot/aperture/window/iris size of the waveguide geometry and the use of a multi-stepped/dielectric-filled waveguide. We changed the sizes of all the transition geometries within the chosen microwave band of transition based on sensitivity, with the goal of getting the least number of reflections and the most transmission within a reasonable fractional bandwidth. We will end the planned software optimization procedure (HFSS, CST-MW Studio, Feko, MATLAB) when we obtain the lowest reflection and highest transmission values for a fair quantity of -10 dB bandwidth. Band-by-band MS-to-RWG Tables (1–13) show the parametric comparison of transitions.

A. Transition Design Formulas

For any band microstrip line and waveguide transition design, the following design equations are used for the analysis:

(i) Microstrip Calculations

The following conventional equations are used for the microstrip analysis [36]:
Effective dielectric constant:

$$\varepsilon_{eff} = \frac{\varepsilon_r + 1}{2} + \frac{\varepsilon_r - 1}{2}\left(1 + 12\frac{h}{w}\right)^{-0.5}. \quad (1)$$

Characteristics Impedance:

$$Z_0 = \frac{60}{\sqrt{\varepsilon_{eff}}}\ln\left(\frac{8h}{w} + \frac{w}{4h}\right); \quad \frac{w}{h} \le 1 \quad (2)$$

$$Z_0 = \frac{120\pi}{\sqrt{\varepsilon_{eff}}\left[\frac{w}{h} + 1.393 + 0.677\ln\left(\frac{w}{h} + 1.444\right)\right]}; \quad \frac{w}{h} \le 1 \quad (3)$$

Microstrip width:

$$W = \frac{c}{f_0}\sqrt{\frac{2}{\varepsilon_r + 1}}, \quad (4)$$

Width of substrate and ground;
$W_{sub.}$ = 9 to 10 times width of microstrip

$$W_{sub.} = 9w \text{ or } 10w. \quad (5)$$

(ii) Rectangular Waveguide Calculations

The conventional rectangular waveguide expressions are used for the rectangular waveguide analysis for the dominant mode TE_{10} mode transmission [37];
Wavelength:

$$\lambda = \frac{c}{f_0}. \quad (6)$$

Dominant modes; $TE_{mn} = TE_{10}$

Cut-off frequency:

$$f_c = \frac{c}{2\sqrt{\varepsilon_r}\mu_r}\sqrt{\left(\frac{m}{a}\right)^2 + \left(\frac{n}{b}\right)^2}, \quad (7)$$

Guided wavelength:

$$\lambda_g = \frac{\lambda}{\sqrt{1 - \left(\frac{f_c}{f_0}\right)^2}}, \quad (8)$$

Waveguide impedance:

$$Z_g = \frac{\eta}{\sqrt{1 - \left(\frac{f_c}{f_0}\right)^2}}; \text{ for TE mode (where } \eta = \sqrt{\frac{\mu}{\varepsilon}}), \quad (9)$$

Waveguide section length:

$$L = \frac{\lambda_g}{4}, \quad (10)$$

Waveguide length:

$$L_{WG} = N\frac{\lambda_g}{4}. \quad (11)$$

(iii) Microstrip Patch Calculations

In most modern microstrip to waveguide transition design the microistrip patch antennas are used as EM energy launcher and receiver. The following microstrip rectangular patch antenna expressions are used for the parameters dimensions estimations [63].
Patch width:

$$W_p = \frac{c}{2f_0}\sqrt{\frac{2}{\varepsilon_r + 1}}, \quad (12)$$

Patch length:

$$L_p = L - 2.\Delta L, \quad (13)$$

$$\text{where, } L = \frac{\lambda_g}{4}, \quad (14)$$

$$\lambda_g = \frac{\lambda_0}{\sqrt{\varepsilon_{eff}}}, \quad (15)$$

$$L = 0.412h\frac{\left(\varepsilon_{eff} + 0.3\right)}{\left(\varepsilon_{eff} - 0.258\right)}\frac{\left(\frac{W_P}{h} + 0.264\right)}{\left(\frac{W_P}{h} + 0.8\right)}. \quad (16)$$

B. Transition Design Steps

All the design steps of the microstrip to rectangular waveguide transitions are implemented using the flow diagram as illustrated in Fig. 3.

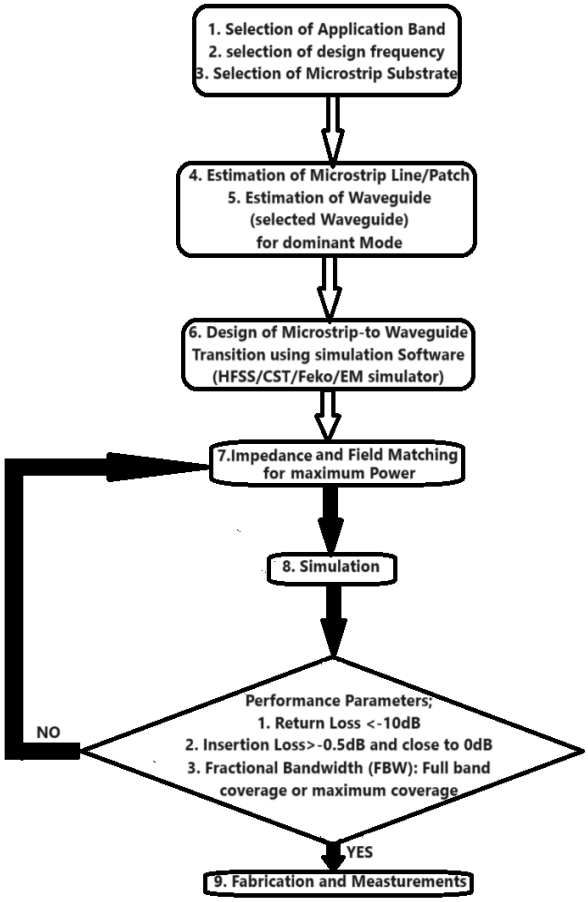

Fig. 3. Flow diagram of design transitions steps

IV. RESULT AND DISCUSSIONS

The transition results have been explained in this section for the complete knowledge of the transitions.

A. Transition Performance Parameters

A microstrip-to-waveguide transition tested for good performance is analyzed in terms of its reflection coefficient/return loss (RL), transmission/coupling coefficient or insertion losses, and -10 dB relative, absolute, and fractional bandwidths [36, 55].

Return Loss: The standing wave ratio (SWR) and the reflection coefficient (Γ) are both related to return loss. A lower SWR leads to an increase in return loss. The metric of return loss measures the effectiveness of matching devices or transmission lines. If the return loss is significant, the match is excellent. We prefer a high return loss because it leads to a smaller insertion loss. A transmission line discontinuity reflects the signal strength relative to the return loss. A mismatch between the line's characteristic impedance and the connected termination or load might create this discontinuity. It is commonly stated as a decibel ratio (dB).

$$\text{Return Loss}\left(\text{dB}\right)=\frac{\text{P}_i}{\text{P}_r}, \tag{17}$$

where P_i is the incident power, P_r is the reflected power and RL (dB) is the return loss in dB. Therefore, RL is a positive. Where P_i is the incident power, P_r is the reflected power and RL (dB) is the return loss in dB. Therefore, RL is a positive quantity, whereas the reflection coefficient is negative [55].

Insertion Loss: The term insertion loss (IL) can also refer to coupling or transmission coefficients. Insertion loss refers to the loss of signal power resulting from the insertion of a device into a transmission line.

$$\text{Insertion Loss}\left(\text{dB}\right)=\frac{\text{P}_t}{\text{P}_r}, \tag{18}$$

where P_r is the power that a load receives after insertion, P_t represents the transmitted power, and IL (dB) represents the insertion loss in decibels.

Bandwidth: In regards to the MS-to-WG transition, three types of bandwidths are in trend, namely, absolute bandwidth, relative bandwidth (RBW), and fractional bandwidth (FBW). Absolute bandwidth is defined as the difference of the frequencies corresponding to the -10 dB points in the return loss curve. Fractional bandwidth is defined as the ratio of the absolute bandwidth to the operating microwave band's center frequency. Relative bandwidth is defined as the ratio of the absolute bandwidth to the operating microwave bands. Mathematically, these three bandwidths are expressed by equations (19) to (21).

$$\text{-10 dB bandwidth }\left(\text{BW}\right)=f_H-f_L, \tag{19}$$

$$\%\text{ Fractional bandwidth}=\frac{f_H-f_L}{f_n}\times 100, \tag{20}$$

$$\%\text{ Relative bandwidth}=\frac{\text{-10 dB bandwidth}}{\text{Target band}}\times 100. \tag{21}$$

B. Return Loss and Insertion loss

Figure 4 displays the return loss and insertion loss plots for the W-band MS-to-RWG transition.

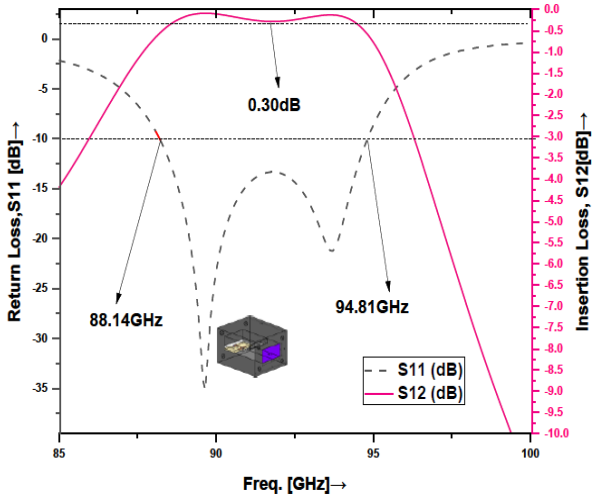

Fig. 4. S-Parameters of W-band MS line-to-RWG transition [60]

The figure shows that the return loss is well below the -10 dB level, while the insertion loss lies between 0 and -0.50 dB. The fractional bandwidth (FBW) for this transition is ∽8% [60].

C. Propagation Constants

The propagation constant (γ) of any electromagnetic wave is given by

$$\gamma = \alpha + j\beta, \quad (22)$$

where, α= Attenuation Constant and β= Phase Constant.

Therefore, the propagation constant provides information about the traveling modes, cutoff frequency, dominant mode, phase constant, and their attenuation constants, as shown in Figs. 5 and 6 [59, 60]. Attenuation values become zero after the cut-off frequency, and the phase constant value starts growing after the cut-off frequency.

The TE10 is the dominant mode of the rectangular waveguide, while the other higher order modes of the waveguides are TE01, TE11, TE20, and TM11 as illustrated in the Figs. 6(b) and 6(c).

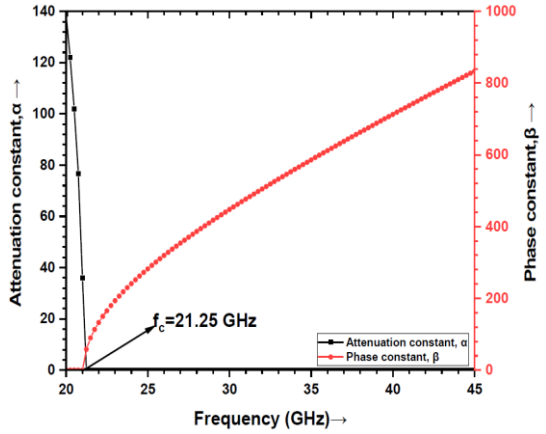

Fig. 5. S-Parameters of W-band MS line-to-RWG transition [59]

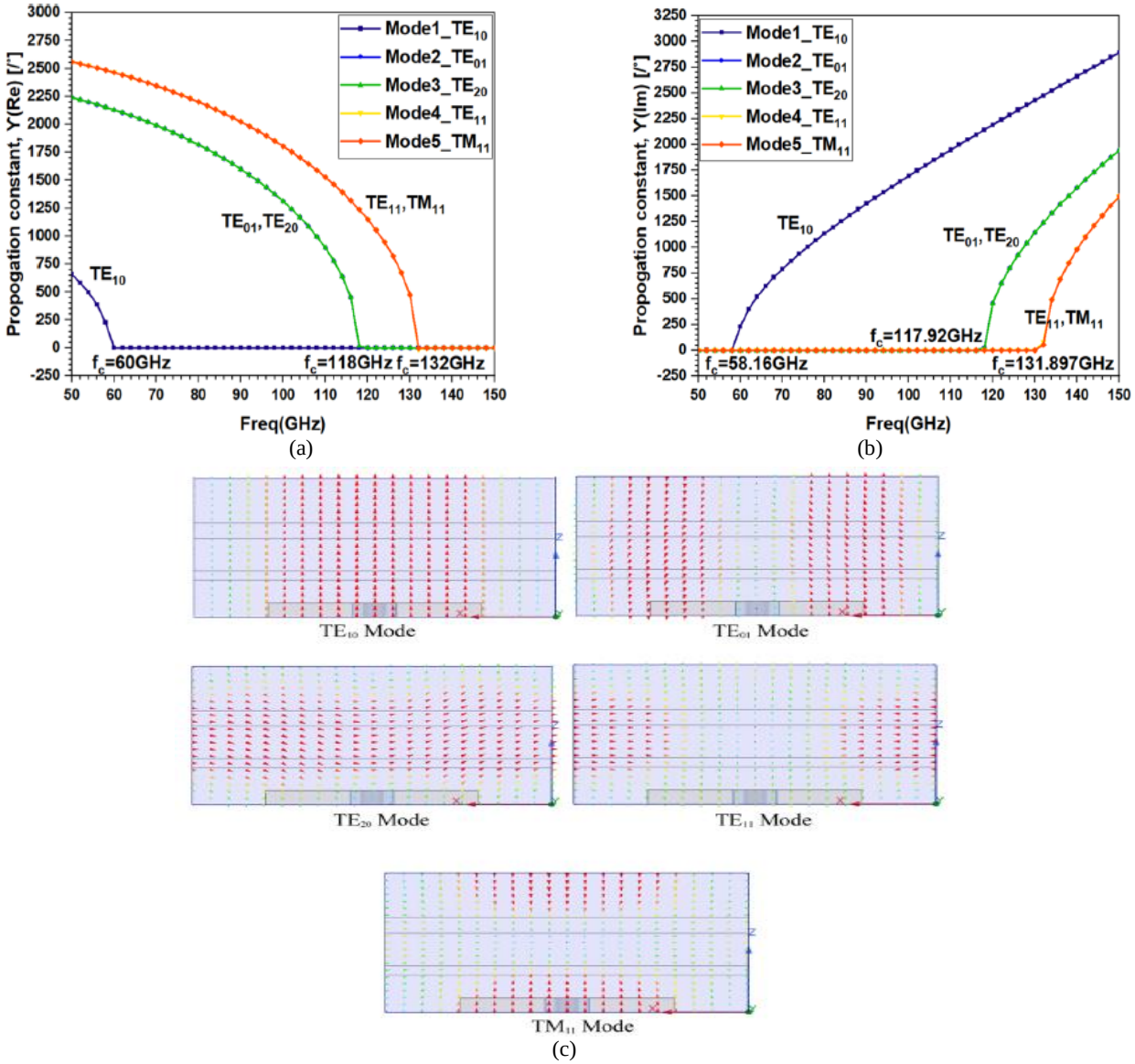

Fig. 6. Different modes of MS-to-WR10 transition: (a) propagation constant (real), (b) propagation constant (imaginary) and (c) different modes of W-band transition [60]

D. Prototype of Microstrip to Rectangular Waveguide Transitions

The prototype models of the microstrip line to rectangular waveguide transitions for W-band and Ka-band are shown in Fig. 7 (a–b).

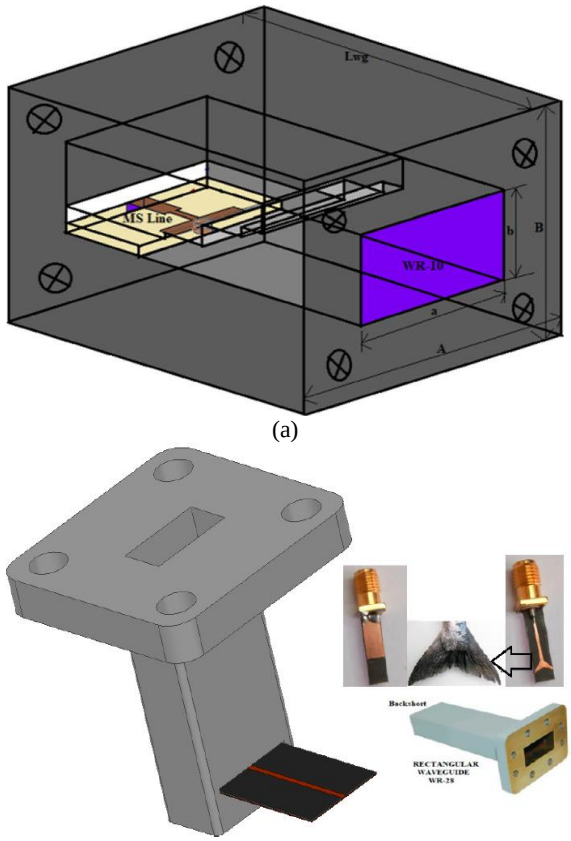

(a)

(b)

Fig. 7. Prototype of MS-toWg transitions (a) W-band [60], and (b) Ka-band [59]

E. The general RLC equivalent of the Transitions

The T-equivalent and π-equivalent circuits are the same for any two-port microstrip line to rectangular waveguide transitions [59]. Check out Figures 8(a) and 8(b) for examples. The researchers can extract these circuits from the knowledge of the simulated S-parameters. The conversion formulas [36] transform the S-parameters into the two-port *Z*-parameters and *Y*-parameters. After that, these equivalent *Z*-parameters are converted into the T-equivalent circuit using equations (23) and (25),

$$Z_A = Z_{11} - Z_{12}, \quad (23)$$

$$Z_B = Z_{12}, \quad (24)$$

$$Z_C = Z_{22} - Z_{12}. \quad (25)$$

Then these T-equivalent impedance values $Z=R+jX_L$ or $Z=R+jX_C$ are compared with $(R+j\omega L)$ or $(R-1/j\omega C)$. Where, $\omega=2\pi f_r$ and f_r is the resonance frequency.

For π-equivalent circuit the *Y*-parameters are converted using the following relationships of Equations (26) to (28),

$$Y_A = Y_{11} - Y_{12}, \quad (26)$$

$$Y_B = -Y_{12}, \quad (27)$$

$$Y_C = Y_{22} - Y_{12}. \quad (28)$$

Then these π-equivalent admittance values $Y=G+jB$ are compared with $(G+j\omega C$ or $(G-1/j\omega L)$. Where, $\omega=2\pi f_r$ and f_r is the resonance frequency.

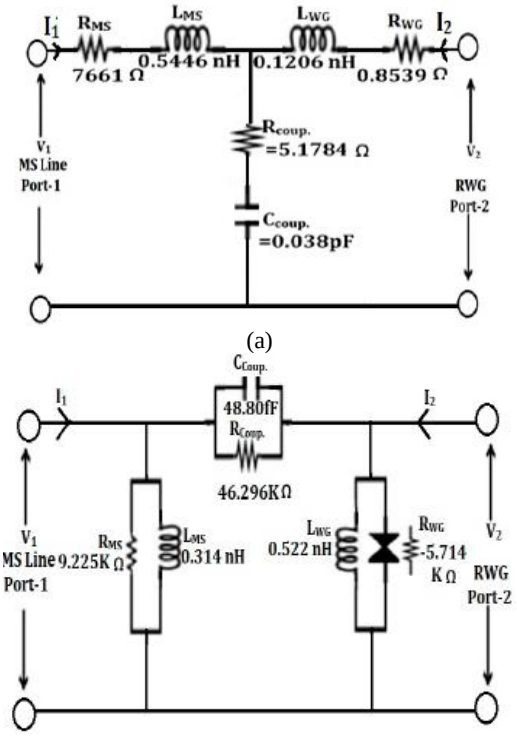

Fig. 8. RLC electric equivalent circuit of E-plane microstrip-to-WR28 Ka-band transitions: (a) T-equivalent circuit, (b) π-equivalent circuit [59]

V. Comparative Study of Transitions

The complete range of microwave bands is generally defined from 300 MHz to 300 GHz [36]. Microwave bands mainly comprise VHF, UHF, SHF, L, S, C, X, Ku, and Ka bands (from 300 MHz to 40 GHz), mm-wave bands, Q, U, V, E, D, and W bands (from 33 GHz to 170 GHz), and submillimetre wave bands (from 170 GHz to 325 GHz) [36]. The microwave bands above 300 GHz normally fall in the THz wave band. In the starting RF frequency bands from 300 MHz to 4 GHz, which mostly comprise VHF, UHF, SHF, L-band, and S-band, the waveguide to coaxial cable connectors and transitions are the most popular ones. However, with the technological advancement and miniaturization of MMIC circuits, devices and components demand new types of low-loss transition compatible with planar circuits. Thus, the development of waveguide to microstrip line interconnects and vice versa is necessarily required, and coaxial transitions fail at these higher frequencies above 10 GHz. Thus, MS-to-WG transitions work well above 4 GHz. A complete coverage of microwave, mm-wave, and THz waves' microstrip line to waveguide transitions from 4 GHz to 325 GHz is illustrated in tables from Table 1 to Table 13.

TABLE 1
C-BAND (4 GHz-8 GHz) TRANSITIONS

Ref.	Substrate Used for MSL	RWG Type (a mm × b mm) and wall Thickness (t mm)	RL <(dB)	IL >(dB)	FBW (%)	Coupling Method and Features	Applications
[4] X. Huang and K.-L. Wu May 2012	Rogers Duroid 5870, ε_r = 2.33 h_1=1.58mm h_2=h3=0.60mm tanδ=0.0012	WR-137 (34.85× 15.80) t=1.625	15	0.30	13.33 (FBW)	. The transition is made up of an open-circuited microstrip quarter-wavelength resonator and a resonant U-shaped slot on the top broadside wall of a short-circuited waveguide . Longitudinal inline (0˚) multi-layered . wide bandwidth . compact in size . convenient for mass production . easy integration of multilayer structure . via less . highly compatible with planar circuits	. In commercial and military communication systems for microwave and mm-wave applications

TABLE 2
X-BAND (8 GHz-12 GHz) TRANSITIONS

Ref.	Substrate Used for MSL	RWG Type (a mm × b mm) and wall Thickness (t mm)	RL <(dB)	IL >(dB)	FBW (%)	Coupling Method and Features	Applications
[2] Y. Ren et al. 2019	F4BM ε_r = 2.65 h=1.58mm tanδ=0.001	WR-90 (22.86 × 10.16) t=1.27	15	0.50	35 (Relative BW)	. . End inserted 90˚ . Inline . Magnetic coupling . uses Impedance transformer . microstrip probe 21 number of complementary split ring resonators (CSRRs) has been loaded in the patches to broaden the bandwidth and increase efficiency . moderate bandwidth . high efficiency . light weight . Economic . small size . simple processing methods	Wireless communication, . radar, . Remote sensing. and . electronic warfare has been operated in microwave and millimeter-wave frequencies
[5] N. Kaneda et al. Dec. 1999	Duroid ε_r = 10.2 h=0.635mm tanδ=0.002 Alumina ε_r = 9.9 h=0.635mm tanδ=0.0002	WR-90 (22.86 × 10.16) t=1.27	12 (Duroid) 15 (Alumina)	0.40 (Duroid) 0.15 (Alumina)	34(Relative BW) (Duroid) 30(Relative BW) (Alumina)	. End inserted (inline 90°) H-Plane . Transition using Quasi-Yagi antenna radiator launcher (antenna), consists of two dipole antennas, a truncated ground plane, and a MS-CPS balun. . The antenna is inserted in the E-plane of the waveguide. . low insertion loss . moderate bandwidth . small size . low-cost fabrication . single layered substrate . Both designs have the same dimensions	. Essential components in many microwaves and millimetre-wave application systems

[8] W. Grabherr and W. Menzel 1992	Duroid ε_{r1} = εr1= 2.3 h1=h2 = = 0.8mm tanδ=0.0009	WR-90 (22.86× 10.16) t=1.27	20	0.50	10-20 (Relativ e BW)	. Transitions utilized an aperture-coupled patch antenna radiating into the waveguide . Small size, simple . easy of fabrication . low bandwidth . no waveguide parts like a λ/4 short-circuited section are necessary on the top of the substrate	. Suitable for mm-wave range.
[18] Ting-Huei Lin, Ruey-Beei Wu 2002	Rogers RT/Duroid 5880 ε_r = 2.2 h=0.7874mm tanδ=0.0009	WR-90 (22.86 × 10.16) t=1.27	15	0.70	35 (FBW)	.E-plane (90°) end launcher . The transition utilized a tapered coplanar strip probe and microstrip-to-slot line transformer, the transition includes three parts: a microstrip-to-slot line transition circuit, a tapered coplanar strip (CPS) probe inserted into the E-plane of the end of the waveguide, and an intermediate section of slot line for impedance matching . Low insertion loss . highly compatible with MIC technology . broad bandwidth . compact size . easy assembly . low fabrication cost	. Play an essential part in specific components like antenna feeds, . high Q filters, . diplexers, . commercial and military systems
[26] Ruei-Ying Fang, and Chun-Long Wang Sep. 2013	Rogers RT/Duroid 5880 ε_r = 2.2 h=0.7874mm tanδ=0.0009	WR-90 (22.86 × 10.16) t=1.27	15	0.30	37.33 and 20.95 (FBW)	. E-plane broadside wall coupled, . Bow-tie Launcher . Transition using capacitance compensated and transition using quarter-wavelength . compact . complex structure . broad bandwidth	. mm-wave receivers and transmitters
[58] A. Varshney et al. 2022	Duroid ε_r = 4.4 h=1.6mm tanδ=0.02	WR-90 (22.86 × 10.16) t=1.27	10	2.1	28 (FBW)	. E-Plane Broad wall inserted (inline 90°) . Elliptical patch antenna and a tapered impedance transformer	. Microwave Laboratory Experiment purposes . Space communications . Satellite Communications . RADAR, . Amateur radio, . As a connector for MMIC/MIC circuits and devices
[62] A. Varshney et al. 2024	Duroid ε_r =4.4 h=1.6mm tanδ=0.02	WR-90 (14× 21.35) t=1.27	20	0.60	100.5 (FBW)	. SIW-MS transition . Four-mitered taper end with two aerodynamic slots .6 via/row	. better choice to interconnect MMIC/MIC/HMIC planer devices, circuits, components, and interconnects of front and transmitter and receivers of satellite and radar communications . SICs and systems, wireless, Satellite, and RADAR applications . X-band and Ku-band

TABLE 3
KU-BAND (12 GHz-18 GHz) TRANSITIONS

Ref.	Substrate Used for MSL	RWG Type (a mm × b mm) and wall Thickness (t mm)	RL <(dB)	IL >(dB)	FBW (%)	Coupling Method and Features	Applications
[14] Zahid Yaqoob Malik et al. Jan. 2010	Rogers's 4350B ε_r = 3.66 h=0.762mm tanδ=0.0037	WR-62 (15.80 × 7.90) t=1.015	14	0.50	9 (FBW)	. End launch, transverse wall (Improved right-angle transition with amplification) . Transition was achieved by passing a portion of a microstrip through an aperture in a transverse wall of a waveguide. . Aperture coupled . no need for waveguide tees or other components . realizable on inexpensive substrates . the assembly directly picks the signal from the antenna and provides an amplified signal for down-conversion	. It can be used for radar systems, . EW systems and compact communication Systems.
[33] Z. Liu, et al. Jan. 2019	Manufactured and designed with different thicknesses of substrates RO4350B ε_r = 3.66 h=0.508mm RT-duroid 5880 h=0.508 mm RT-duroid 5880 h=0.254 mm	WR-62 (15.80 × 7.90) t=1.015	21	0.415	61.67 (Relative BW)	. Back-to-back Inline MS line to empty SIW transition . Dielectric taper has been eliminated in SIW . broad BW . low attenuation has been achieved by introducing air cut in empty SIW . the simple and planar structure . no need for a dielectric taper . broad bandwidth	. Successfully applied to design various microwave and mm-wave passive components, such as filters, phase shifters, directional couplers horn antenna, etc. . Integrate ESIW circuits with active devices such as amplifiers

TABLE 4
K-BAND (18 GHz-26 GHz) TRANSITIONS

Ref.	Substrate Used for MSL	RWG Type (a mm × b mm) and wall Thickness (t mm)	RL <(dB)	IL >(dB)	FBW (%)	Coupling Method and Features	Applications
[1] E. Hassan et al. 2019	RO4350B ε_r = 3.66 h=0.254mm	WR-42 (10.67 × 4.32) t=1.015	15	1.3	10 (Relative BW)	. Inline (0˚) . Signal coupling between an MSL and an RWG by optimizing the distribution of copper in two design domains . compact . most cost-effective . excellent shielding . low attenuation . low bandwidth .two layered PCB	. Using standard PCB technology, the transition can be directly used to integrate into the sensor at the lowest possible cost

[13] J. H.C. Van Heu-ven March 1976	Silica ε_r = 3.8 h=0.5mm	WR-42 (10.67 × 4.32) t=1.015	26	0.25	46 (Relative BW)	. End inserted (Inline) E-plane (90°) . The basic idea is the use of gradually tapered ridges at opposite sides of a dielectric substrate, concentrating and rotating the electrical field into a parallel line. . The symmetrical line is matched by a balancing transformer (balun) to the asymmetrical microstrip. An outline of the substrate is inserted into the waveguide. The ridges and the ground plane of the microstrip are connected to the wall of the guide along the line length . low reflection . low attenuation . wide band . reproducible performance . sensitive to small variations in the dimensions	. Especially useful at frequencies above 10 GHz.
[21] Aliak-barian et al. 2010	Three Substrates RT5880 ε_r = 2.2 h_1=0.7874mm RO4003 ε_r = 3.38 h_1=0.508mm RT6010 ε_r = 10.2 h_1=1.27mm	WR-51 (12.95 × 5.7) t=1.27	16	4.0	31.5 (RT5880) 15 (RO4003) 4.5 (RT6010) (FBW)	. End-wall slot coupling, waveguide splitter and three-port . It consists of an end-wall connection between a simple metal waveguide and a double-sided etched substrate. There is a double slit in the ground of the substrate, coupling the wave to two microstrip ports. Also, two stubs are added to the microstrip line. . easy manufacturing structure . low cost . small size . less complex . wideband bandwidth . non-tilted pattern	. The transition is applied to a dual-band 1 ×2 array and is Suitable for use in series-fed microstrip arrays

TABLE 5
KA-BAND (26 GHz-40 GHz) TRANSITIONS

Ref.	Substrate Used for MSL	RWG Type (a mm × b mm) and wall Thickness (t mm)	RL <(dB)	IL >(dB)	FBW (%)	Coupling Method and Features	Applications
[3] J. Li et al. April 2012	RT-Duriod 5880 ε_r = 2.2 h=0.254mm tanδ≈0.0009	WR-28 (7.112 ×3.556) t=1.015	11	0.95 and 1.94	33 (Relativ e BW)	. Narrow wall b, . side inserted magnetic coupling . Transition utilized a semicircular microstrip ring and stepped impedance transformer.	. They are widely applied in Components and systems of communication, . satellite communication, and military appliance (e.g., millimeter wave transmitter/ receiver components, . Front-end of receivers and vector modulators), . radar, remote sensing, . electronic warfare . Microwave measurement.

[6] Y. C. Shih et al. 1988	RT-Duriod 5880 ε_r = 2.2 h=0.254mm tanδ≈0.0009	WR-28 (7.112 × 3.556) t=1.015	15	0.4	40 (F BW)	. Broadside wall inserted right-angled (90°) . Microstrip probe inserted into the broad wall of waveguide through aperture cut and impedance transformer . simple . compact . low insertion loss . wide bandwidth	. Useful for devices and circuits characterization of MICs and MMICs
[10] Dominic Desla-ndes and Ke Wu Feb. 2001	RT-duriod ε_r = 2.33 h=0.254mm tanδ≈0.00031	WR-28 (7.112 × 3.556) t=1.015	45	0.30	12.67 (FBW)	. Inline H-plane . the microstrip line and rectangular waveguide are fully integrated on the same substrate, and they are interconnected via a simple taper, via holes and metalized grooves . direct integration . small size . low loss . uses via holes . metalized grooves . low radiation losses due to thin substrate . increase conductor losses due to the height of the waveguide reduced	. It can be used to integrate passive waveguide components with MIC and MMIC active circuits
[12] Seema Tomar et al. Dec. 2010	RT-Duriod 5880 ε_r = 2.2 h=0.127mm tanδ≈0.0009	WR-28 (7.112 × 3.556) t=1.015	32	0.70	36 (Relativ e BW) 14.54 (FBW)	. Broadside wall probe insertion through aperture (E-plane) . The probe extends from an extension of a printed microstrip circuit (of active and passive circuits) through an aperture in the broad wall of a short-circuited waveguide . low insertion loss . good return loss . moderate bandwidth . IC/MMIC compatibility . low-cost substrate . via less . feeding without balun	. The transition is MIC/MMIC compatible
[18] Ting-Huei Lin, Ruey-	Rogers RT/Duroid 5880 ε_r = 2.2 h=3.937mm tanδ=0.0009	WR-28 (7.112 × 3.556) t=1.015	15	1.20	40 (FBW)	. E-plane (90°) end launcher . The transition utilized a tapered coplanar strip probe	. Play an essential part in specific components like antenna feeds, . high Q filters,

Beei Wu 2002						and microstrip-to-slot line transformer, the transition includes three parts: a microstrip-to-slot line transition circuit, a tapered coplanar strip (CPS) probe inserted into the E-plane of the end of the waveguide, and an intermediate section of slot line for impedance matching . Low insertion loss . highly compatible with MIC technology . broad bandwidth . compact size . easy assembly . low fabrication cos	. diplexers, . commercial and military systems
[20] Yu Lou et al. May 2008	RT-Duriod 5880 ε_r = 2.2 *h*=0.254mm tanδ≈0.0009	WR-28 (7.112 × 3.556) *t*=1.015	40	1.2 to 2.0	69 (Relative BW) 29.39 (FBW)	. Inline E-plane (90°) . Radial-shaped probe for field matching and extended ground, notch cut on the strip as impedance matching section . double layered PCB . low insertion loss . compact size . low cost . easy to fabricate the printed structure . wideband bandwidth	. Microwave and millimeter circuits or systems
[23] Tang, C. et al. Jan. 2020	RT-Duriod 5880 ε_r = 2.2 *h*=0.127mm tanδ≈0.0009	WR-28 (7.112 × 3.556) *t*=1.015	16.6	0.13	48.3 (FBW)	. Inline (90°) transition . End-wall probe transition using a semicircular loop (impedance transformer), is placed at the E-plane of the rectangular waveguide. . small size . compact . wider bandwidth . ease to fabricate	. RF-front end at mm-wave frequencies
[25] Varshney A. K. Aug. 2013	RT-Duriod 5880 ε_r = 2.2 *h*=0.127mm tanδ≈0.0009	WR-28 (7.112 × 3.556) *t*=1.015	40	0.30	38 (Relative BW)	. E-plane probe inserted . Impedance transformer-based back short transition . simple . compact . mass production	. mm-wave receivers and transmitters

						. via-less	
[32] Cun Long, Li, et al. Dec. 2019	RT-Duriod 5880 ε_r = 2.2 *h*=0.254mm tanδ≈0.0009	WR-28 (7.112 x 3.556) *t*=1.015	13	0.40	71.43 (Relative BW) 30.3 (FBW)	. Inline (0°) . employs a circular patch above a wedge-shaped cavity . low cost . prototype . single-sided PCB . wideband . compact structure and easy integration . high integration density	. Millimeter wave applications
[38] R. Gupta, P. P. Kumar Feb. 2020	Aluminium alloy Al6061	WR-28 (7.112 × 3.556) *t*=1.015	23.4	0.47	38 (Relative BW)	.90° waveguide to coaxial . Field matching and Impedance matchings were achieved through a ridged waveguide, customized coaxial probe and back-short distance . compact and light weight . small size . < 1W power handling . improved RF leakage of < -88dBm	. In military and space-borne electronic systems
[39] Y. Tahara, et al. 2005	Conductor-backed substrate ε_r = 2.2	WR-28 (7.112 × 3.556) *t*=1.015	15	NA	5 (FBW)	. E-plane vertical (90˚) broad wall aperture cut .MS is fabricated on the single-layered PCB . No need for WG back- short . mushroom-like electromagnetic band gap (EBG) is used instead of WG back-short . low profile transition . EBG structure provides a high impedance surface. . Impedance matching is accomplished with microstrip impedance steps at the feed points . EBG patches and MS probes are on the same surface . Easy fabrication	. Microwave and mm-wave applications

[57] A. Varshney, et. al. 2022	RT-Duriod 5880 ε_r = 2.2 h=0.127mm tanδ≈0.0009	WR-28 (7.112× 3.556) t=1.015	34	0.10	72 (FBW)	. E-plane probe inserted . Impedance transformer-based back short transition . simple . compact . mass production . via-less	. modern mobile devices such as smartphones
[59] A. Varshney, et. al. 2023	RT-Duriod 5880 ε_r = 2.2 h=0.127mm tanδ≈0.0009	WR-28 (7.112× 3.556) t=1.015	20	0.50	66.15 (FBW)	. Broadside wall inserted, . E-plane, .90˚ fishtail shaped probe insertion, . compact, easy fabrication of PCB	. K-band (23.52 GHz to 26 GHz), Q-band (33 GHz to 45 GHz), and U-band (40 GHz to 45 GHz)

TABLE 6
Q-BAND (33 GHz-50 GHz) TRANSITIONS

Ref.	Substrate Used for MSL	RWG Type (a mm × b mm) and wall Thickness (t mm)	RL <(dB)	IL >(dB)	FBW (%)	Coupling Method and Features	Applications
[6] Y. C. Shih et al. 1988	RT-Duriod 5880 ε_r = 2.2 h=0.254mm tanδ≈0.0009	WR-15 (3.76 × 1.88) t=1.015	15	0.60	17.24 (FBW)	. Microstrip probe inserted into the broad wall of waveguide through aperture cut and impedance transformer . simple . compact . low insertion loss . wide bandwidth . Broadside wall inserted right-angled (90°)	. Useful for devices and circuits characterization of MICs and MMICs
[9] F. J. Ville-gas et al. Jan. 1999	Alumina ε_r = 9.9 h=0.127mm tanδ≈0.006	WR-15 (3.76 × 1.88) t=1.015	15	0.35	11 (FBW)	. Broadside E-plane right-angled (90°) . a single-layer substrate . new matching topology . new cavity enclosure . hermetic sealing of the interface . low-cost . New design methodology based on iris coupling implementation . more affordable . package-integrable transitions	. Amplifiers and transceivers in military and commercial systems, . especially for millimeter-wave (mm-wave) applications.
[31] Simone et al. Feb. 2018	Alumina 98% ε_r = 9.8 h=0.127mm tanδ≈0.006	WR-22 (5.69 × 2.84) t=1.015	24	0.26	40 (Relative BW)	. Inline end launcher transition . Transition used a section of the ridged waveguide and Chebyshev impedance transformer. . A simple small patch is matched to the waveguide through a ridged configuration, on which the patch is shorted and a Chebyshev impedance transformer provides the matching from the ridge to the full waveguide. . The impedance match was obtained using a section of ridged waveguide with stepped ridges . the simple and planar structure . increases the ease of fabrication and the compactness . good return loss . via-less . broad BW	. Q-band (33–50 GHz) receiver of the Sardinia Radio Telescope

TABLE 7
U-BAND (40 GHz-60 GHz) TRANSITIONS

Ref.	Substrate Used for MSL	RWG Type (a mm × b mm) and wall Thickness (t mm)	RL <(dB)	IL >(dB)	FBW (%)	Coupling Method and Features	Applications
[46] S. Kumari 2017	RT-Duriod 5880 ε_r = 2.2 h=0.127mm	WR-19 (4.7752 × 2.3876) t=1.015mm	20	0.27	40	. E-plane probe along length . Monopole antenna as probe . symmetrical ground sleeves	. radar systems . utilized in millimeter wave communication systems in U-band . Future in astrophysics, or atmospheric sounding and remote sensing.

TABLE 8
V-BAND (50GHz-75GHz) TRANSITIONS

Ref.	Substrate Used for MSL	RWGType (a mm × b mm) and wall Thickness (t mm)	RL <(dB)	IL >(dB)	FBW (%)	Coupling Method and Features	Applications
[6] Y. C. Shih et al. 1988	RT-Duriod 5880 ε_r = 2.2 h=0.127mm tanδ≈0.0009	WR-12 (3.10 × 1.55) t=1.015	12	1.0	40 (Relative BW)	. Microstip probe inserted into the broad wall of waveguide through aperture cut and impedance transformer. simple . compact . low insertion loss . wide bandwidth . Broadside wall inserted right-angled (90°)	. Useful for devices and circuits characterization of MICs and MMICs
[21] Aliak-barian et al. 2010	Rogers RT/Duroid 5880 ε_r = 2.2 h=0.254mm tanδ=0.0009	WR-15 (3.76 × 1.88) t=1.015	17	4.0	37.7 (FBW)	. End-wall It consists of an end-wall connection between a simple metal waveguide and a double-sided etched substrate. There is a double slit in the ground of the substrate, coupling the wave to two microstrip ports. Also, two stubs are added to the microstrip line. . slot coupling, waveguide splitter and three-port . easy manufacturing structure . low cost . small size . less complex . wideband bandwidth . non-tilted pattern	. The transition is applied to a dual-band 1 X2 array and is Suitable for use in series-fed microstrip arrays
[56] A. Varshney, et. al. 2022	InP , ε_r = 2.2 h=50µm tanδ=0.0001	WR-15 (3.76 × 1.88) t=1.015	30	0.09	40.76 (Relative BW)	. Dipole antipodal antenna as launcher . Double-sided etched InP substrate	. mm-wave communication interconnects for the front end in receivers/ transmitters, MMIC/MIC circuits, unlicensed devices (59–64 GHz), the ISM band (61.25 GHz _ 0.25 GHz), Earth exploration satellites, Inter-SAT

TABLE 9
E-BAND (60 GHz-90 GHz) TRANSITIONS

Ref.	Substrate Used for MSL	RWG Type (a mm × b mm) and wall Thickness (t mm)	RL <(dB)	IL >(dB)	FBW (%)	Coupling Method and Features	Applications
[7] W. Grapher et al. Sept. 1994	Alumina ε_{r1} = 9.8 h_1=0.154mm tanδ=0.006 Fused Quartz ε_{r2} = 3.75 h_2=0.11mm for radiating element	WR-12 (3.10 × 1.55) t=1.015	15	0.30	10 (FBW)	. Broadside wall inserted (90°) . Slot-coupled microstrip antennas radiating into the waveguide . low bandwidth . compact . small size	. This type of transition is suited for mm-wave system applications for example, in traffic applications.
[15] Sakakibara, K. et al. 2008	Teflon (top and bottom layers) ε_r = 3.48 h=0.127mm tanδ=0.0035 Adhesive substrate (Middle Layer) ε_r = 3.54 h=0.127mm tanδ=0.004	WR-10 (2.54 × 1.27) t=1.015	20	0.71	32.5 (Relative BW)	. End inserted probe transition (90°) . The transition was developed by applying a multi-layer substrate to remove the upper back-short waveguide on the substrate. . A probe at one end of the microstrip line is inserted into the waveguide whose one end is short-circuited . multi-layered . uses via holes . flat and planar transition . broad bandwidth . system and cost of millimeter-wave device will gradually decrease	. Millimeter-wave wireless applications, . Automotive radar system (most cars will equip this), . broadband and Gbit high-speed wireless communication systems whose performance can exceed MIMO and UWB systems in the microwave band, . for connection between waveguide and RF circuit or antenna module.
[27] Azzemi Ariffin et al. May 2016	Liquid Crystal Polymer (LCP) ε_r = 3.16 h=0.10mm tanδ=0.0045	WR-12 (3.10 × 1.55) t=1.015	20	1.41	61.9 (Relative BW)	. Wideband 90° transition . Transitions using the radial probe and extended GND planes . simple probe . wideband bandwidth . uses via-holes	. Broadband ultra-high-speed wireless communication systems such as . Broadband radio links for the backhaul networking of cellular base stations, . Giga wireless LAN, . Gigabit Ethernet networks, . 77GHz automotive RADAR systems and . Inter-vehicle communications

TABLE 10
W-BAND (75 GHz-110 GHz) TRANSITIONS

Ref.	Substrate Used for MSL	RWG Type (a mm × b mm) and wall Thickness (t mm)	RL <(dB)	IL >(dB)	FBW (%)	Coupling Method and Features	Applications
[6] Y. C. Shih et al. 1988	RT-Duriod 5880 ε_r = 2.2 h=0.127mm tanδ≈0.0009	WR-10 (2.54 × 1.27) t=1.015	15	1.0 to 2.0	40 (FBW)	. Microstrip probe inserted into the broad wall of waveguide through aperture cut and impedance transformer . Simple . compact . low insertion loss . wide bandwidth . Broadside wall inserted right-angled (90°)	. Useful for devices and circuits characterization of MICs and MMICs
[9] F. J. Ville-gas et al. Jan. 1999	Quartz ε_r = 4.7 h=0.127mm tanδ≈0.0002 and Fused Silica ε_r = 3.8 h=0.127mm tanδ≈0.00015	WR-10 (2.54 × 1.27) t=1.015	15 (Quartz) 15 (Fused Silica)	0.30 (Quartz) 0.20 (Fused Silica)	12 (Quartz) (FBW) 11 (Fused Silica) (FBW)	. Broadside E-plane right-angled (90°) . a single-layer substrate . new matching topology . new cavity enclosure . hermetic sealing of the interface . low-cost . New design methodology based on iris coupling implementation . more affordable . package-integrable transitions	. Amplifiers and transceivers in military and commercial systems, . especially for millimeter-wave (mm-wave) applications.
[11] Jose M. Pérez-Escu-dero et al. Sep. 2020	Rogers CuClad 233 ε_r = 2.35 h=0.100mm tanδ≈0.0009	WR-10 (2.54 × 1.27) t=1.015	15	0.50	77 (Relative BW)	. Based on ridge and groove gap waveguides . Transition utilizes a multi-section (each of length λ/4) Chebyshev transformer implemented in groove gap waveguide section . Inline, H-plane cut along the length of groove gap RW . simpler and easier to manufacture . no microstrip line taper is required . the microstrip substrate does not enter the bed of the nail area . wide bandwidth . no need for soldering . uses a bed of pin nails	. Uses for sub-millimeter and millimeter frequency applications
[16] B.D. Nguyen et al. Dec. 2005	Alumina ε_r = 9.18 h=0.127mm tanδ=0.0045 Gold metallization =1.5μm	WR-10 (2.54 × 1.27) t=1.015	23	0.60	12 (FBW)	. E-mode coupling-based transition developed by inserting a small microstrip disk sector antenna inside a standard W-band waveguide . End launch, transverse wall (right angle transition) . small compact size . low insertion loss . narrow bandwidth . no need for a quarter-wave transformer	. Often used for antenna or filter design, . for connecting the different parts of circuits.

[17] Earl R. Murphy et al. June 1984	Cuflon substrate ε_r = 2.2 *h*=0.127mm tanδ=NA	WR-10 (2.54 × 1.27) *t*=1.02	23	0.20	23 (FBW)	. Transition is designed by passing a portion of a microstrip circuit through an aperture in a transverse wall of a waveguide . E-plane (Right angle) . compact . simple geometry . low loss	Transition suitable for use in millimeter wave circuits.
[19] Hiedo Ijuka et al. April 2002	Duroid RT 5880 substrate ε_r = 2.2 *h*=0.127mm tanδ=0.0001	WR-10 (2.54 x 1.27) *t*=1.015	40	0.30	7 (FBW)	. E-plane end inserted uses via-holes for electrical connection between conductor strip and ground through single-layered substrate . E-plane end inserted . wide bandwidth . low cost, low profile . no waveguide back short . uses via holes . easy fabrication	.The millimeter-wave application for front end module for an automotive radar sensor, . Suitable for connection between mm-wave components such as an antenna, an amplifier, and a switch having an interface of a microstrip line or a waveguide.
[22] R. Shireen et al. 2010	99.6% alumina ε_r =9.8 *h*=0.100mm tanδ=0.002	WR-10 (2.54 × 1.27) *t*=1.015	30	1.15	75 (Relative BW)	. Back-to-back transition uses an integrated probe for direct coupling to the WR-10 waveguide with the use of metalled vias on both sides of the microstrip line. probe insertion through an inverse T-shaped aperture cut in the broad wall of the waveguide . End-wall (inline) . uses large numbers of vias . wide BW . planar structure	. Widely used for wireless communications, . RADAR sensors and imaging receivers at mm-wave frequencies
[24] Ziqiang Tong, Andreas Stelzer May 2012	Taconic TLE-95 ε_r = 2.95 *h*=0.127mm tanδ=0.004	WR-10 (2.54 × 1.27) *t*=1.015	20	0.50	48.5 (Relative BW)	. A differential microstrip patch antenna (DMPA) inside the waveguide acts as a radiation element. . Vertical transition . uses vias holes . compact size and . simple fabrication . allow mass production . wide bandwidth	. Suitable for numerous mm-wave applications
[28] J. M. Pérez April 2016	Cyclic-Olefin Copolymer (Topas TM) COC ε_r = 2.34 *h*=0.100mm tanδ=0.0019	WR-10 (2.54 × 1.27) *t*=1.015	19.4	0.50	82.5 (Relative BW)	. . Transition operating in the full W-band . Chebyshev multisession (each of length λ/4) transformer . Linear taper transformer in MS line . Inline (0°) transition . simple . compact . mass production . low insertion loss . no soldering is required . wide bandwidth . there is no need to optimize transition parameters	. W-band for applications in different fields as imaging, . communication, . RADAR or automotive RADAR

[30] Pérez-Escu-dero et al. Sep. 2018	Rogers Cuclad εr = 2.4 h=0.100mm tanδ=0.0019	WR-10 (2.54 x1.27) t=1.015	15	0.63	32 (Relative BW)	. Chebyshev multi-section transformer and microstrip linear taper . Inline transition . simple . easy to manufacture . planar structure . increases the ease of fabrication and integration . narrow BW	. Imaging, . Communications, . RADAR and automotive RADAR
[35] A. Meyer et al. April 2020	Rogers 3003 εr = 3.0, h =0.127 mm	Dielectric Filled WG WR-10 (2.54×1.27) t=1.015	18	0.49	28 (Relative BW)	. Microstrip line to circular dielectric waveguide.90° broadband stacked-patch transition . An MSL-to-DWG transition with dual-polarized feeding using a stacked patch topology . The stacked patch is inserted into a dielectric stamp at the bottom of the DWG that increases coupling efficiency . fundamental mode HE_{11}^{x} and HE_{11}^{y} in a DWG . Interconnect data speeds are doubled. . Interconnect data speeds are doubled. PCB space requirements are minimal. . There is no need for any extra steel guiding structures. Efficient coupling increase. . IL and RL are horrible. . Cross talk has been reduced in value. . PCB with only one layer	.A critical component for high data rate transmission
[52] Y.C. Leong and S. Weinreb 1999	i)Teflon-127 εr = 2.2, h =0.127 mm ii) Die16-127 εr = 6.0, h =0.127 mm iii) Alumina-100 εr = 10.1, h =0.100 mm iv) GaAs-100 εr = 13.0, h=0.100 mm	WR-10 (2.54×1.27) t=1.015	20	1.5 0.1(Teflon) 0.24(Alumina)	27 (FBW)	. Broadside probe (Design-1) And Longitudinal Probe (Design-2) . E-plane vertical . Stepped Probes as launchers . simple structure . ease of fabrication . single layer PCB . Excellent Noise performance with alumina substrate . uses waveguide back-short	. Microwave and mm-wave communications, . Automotive and tracking Radar . Microwave Imaging systems
[60] A. Varshney, et al. 2023	Roger RT Duroid 5880 h:0.127mm tanδ=0.0009	WR-10 (2.54 × 1.27) t=1.015	38	0.09	19.05% (Absolute BW)	. Inline . Uses four $\lambda g/4$ waveguide ridge sections (a multi-section Chebyshev WG transformer is used) . 4 RWG ridge sections	. planarMMIC /HMIC/MIC circuits and systems interconnects, mm-wave applications, . as a connector for multiple device characterization is built-in planar technology in waveguide-based equipment, . RADAR and satellite front-end transmitter/receiver systems in W-band

TABLE 11
D-BAND (110 GHz-170 GHz) TRANSITIONS

Ref.	Substrate Used for MSL	RWG Type (a mm × b mm) and Wall Thickness (t mm)	RL <(dB)	IL >(dB)	FBW (%)	Coupling Method and Features	Applications
[34] P. Hügler, et al. Feb. 2020	RO3003 ε_r=3.0, h=0.254 mm	WR-6 (1.70 × 0.83) t=0.99	10	1.2, 1.8	25 (Relative BW)	. DMSL to waveguide is built for a mixed multilayer PCB consisting of three substrates with the thicknesses of 127, 254, and 500 μm . Inline (0°) H-plane, end inserted differential MSL-to-WG transitions . multi-layered PCB . complex design . costly . uses via holes	. Specially applicable at mm-waves applications . These layers could also be used for digital signals or power planes in future designs
[47] Hassona, A 2018	SiC ε_r=9.66 h=0.075mm tanδ=0.003	WR-6 (1.70 × 0.83) t=0.99	10	2.0 and 0.67 (min.)	22.85 (FBW)	. E-plane interconnect realized using a unilateral inline structure . No need for any galvanic contacts and any special processing . low-loss . wide-bandwidth	. mm-Wave systems . can be used in any MMIC technology
[48] Hassona, A., et al.2020	Roger's RO4350B ε_r =3.48 h=0.45mm tanδ=0.0037	WR-6 (1.70 × 0.83) t=0.99	10	2.0	17.14 (-3dB FBW)	. Transition used an eWLB packaging technology . For suppressing parallel plate modes and minimizing field leakage transition utilizes an EBG structure . mushroom-shaped EBG patches are used to suppress field leakage in undesired directions . drawback of the transition is that an air gap is present between the eWLB surface and the waveguide opening	. mm-Wave systems . can be used in any MMIC technology
[49] Xu,W., et al. 2016	Roger RT Duroid 5880 h:0.127mm tanδ=0.0009	WR-6 (1.70 × 0.83) t=0.99	10	0.13	42 (-3dB FBW)	. E-plane probe transition . Simple . Easy to integrate and fabricate . Single layered PCB . Compact and low cost.	. Suitable for mm-wave applications
[50] Hassona, A., et al. 2017	Roger's RO4350B ε_r =3.2 h:0.45mm tanδ=0.0037	WR-6 (1.70 × 0.83) t=0.99	10	3.0	22 (-3dB FBW)	. Interconnection is achieved through the use of embedded wafer-level ball grid array (eWLB) packaging technology . An EBG structure is used in the transition to suppress parallel plate modes and reduce field leakage. . Also uses Ball grid arrays (BGAs). . Mushroom-type EBG is fabricated in two two-layer substrates.	.mm-wave MMIC interconnects beyond 100GHz

[51] Hassona, A., et al. 2017	Roger's RO4350B ε_r =3.2 *h*:0.45mm tanδ=0.0037	WR-6 (1.70 × 0.83) *t*=0.99	10	3.4	26 (-3dB FBW)	. transition realize using slot antenna . utilized eWLB packaging process is suitable for low-cost high-volume production and allows heterogeneous integration with other technologies . cost-effective . multi layered PCB	. mm-Wave systems . can be used in any MMIC technology
[61] A. Varshney, et al. 2022	Roger RT Duroid 5880 ε_r =2.2 *h*:0.127mm tanδ=0.0009	WR-7 (1.651 × 0.8255) *t*=0.127	10	1.8	18.5 (FBW)	. Multi-Step (5) Impedance Transformer	. most suitable for mm-wave communication, . interconnects for front end in receivers/transmitters, MMIC, MIC circuits
	Roger RT Duroid 5880 *h*:0.127mm tanδ=0.0009	WR-7 (1.651 × 0.8255) *t*=0.127	10	0.92	10.6 (FBW)	Three-Step Impedance Transformer	. most suitable for mm-wave communication, . interconnects for front end in receivers/transmitters, MMIC, MIC circuits
	Roger RT Duroid 5880 *h*:0.127mm tanδ=0.0009	WR-7 (1.651 × 0.8255) *t*=0.127	10	1.73	5.02 (FBW)	Using PIN Diode (ON State)	. most suitable for mm-wave communication, . interconnects for front end in receivers/transmitters, MMIC, MIC circuits
	Roger RT Duroid 5880 *h*:0.127mm tanδ=0.0009	WR-7 (1.651 × 0.8255) *t*=0.127	10	1.48	3.6 (FBW)	Using resister	. most suitable for mm-wave communication, . interconnects for front end in receivers/transmitters, MMIC, MIC circuits

TABLE 12
G-BAND (140 GHz-220 GHz) TRANSITIONS

Ref.	Substrate Used for MSL	RWG Type (*a* mm × *b* mm) and wall Thickness (*t* mm)	RL <(dB)	IL >(dB)	FBW (%)	Coupling Method and Features	Applications
[41] M. Somnath et al. 2020	Quartz substrate ε_r = 3.8, *h*=0.075 mm tanδ = 0.0001 at 500 GHz Gold as metallization h_{gnd}=0.05mm	WR-5 (1.295 × 0.647) *t*=0.635mm	18	0.31	41.66 (FBW)	. transition using an extended longitudinal E-Plane probe . wide operating band . low-loss . Transition has a comb-like structure which enables it to have broadband characteristics. . low-complexity, . low-profile . Compact . Easy Fabrication	. for sub-mm-wave/lower THz applications

[42] O. Donadio et al. 2011	semi-insulating gallium arsenide (SI-GaAs) ε_r = 12.9 *h* =0.630mm to 0.050 mm tanδ = 0.0001	WR-5 (1.30 × 0.66) *t*=0.635mm	10	4.0	27.77	. E-plane probe, used in the transition No need for any extra matching network . back-to-back configuration . The substrate is parallel to the E-field and is aligned along the direction of propagation of the waveguide . The housing was fabricated in split blocks of brass using a CAT-3D computer-numerically-controlled (CNC) milling machine. Standard MIL-F-3922-67B flanges . reduced size and reduced costs in fabrication and assembly	. elevated probe is suitable for direct integration with monolithic microwave integrated circuits
[43] E. Daniel et al. 2002	Alumina (MS-to-WG) ε_r = 9.8 *h*=0.0508mm CuFlon (copper on Teflon@ from Polyflon) ε_r = 2.2 *h*=0.0508mm (For WG-to-antipodal Fin line)	WR-5 (1.30 × 0.66) *t*=0.635mm	10	1.1 (alumina) 1.3 (Teflon) @165GHz	24.25	. Two MMIC-waveguide transitions: E-plane probe and antipodal fin line	. For THz frequency mixers and Amplifiers
[44] A. Tessmann et al. 2006	Quartz substrate ε_r = 3.8, *h* =0.050 mm tanδ = 0.0001 at 500 GHz Gold as metallization h_{gnd}=0.05mm	WR-5 (1.30 × 0.66) *t*=0.635mm	12	2.9 (Back-to-back) <1.5 (Single Transition)	44.44	. back-to-back configuration .longitudinal mounted case . quartz substrate enters the waveguide through a window on the longer side of the waveguide	. 220 GHz Low-Noise Amplifier Modules for Radiometric Imaging Applications . G-band radiometer system used to generate passive millimetre-wave images
[45] H. Aliakbarian et al. 2014	Rogers 5880 ε_r = 2.22 *h*= 0.064 mm	WR-4 (1.09 × 0.56) *t*=0.51mm	10	2.5	27.77	. fully micro-machined double-slot grounded coplanar waveguide (GCPW) to rectangular hollow waveguide transition . radiation loss has been minimized . reduce the coupling insertion loss	. MM-wave and Sub-mm wave applications

TABLE 13
Y-BAND (220 GHz-325 GHz) TRANSITIONS

Ref.	Substrate Used for MSL	RWG Type (*a* mm × *b* mm) and wall Thickness (*t* mm)	RL <(dB)	IL >(dB)	FBW (%)	Coupling Method and Features	Applications
[40] K. Y. Li and Y.H. Cheng	Rogers RO5880 ε_r = 2.22, tanδ = 0.0009 at 10 GHz *h*= .127mm)	WR-3 (0.86 × 0.43) *t*=0.385	10	3.6	28.57 (Relative BW) 11(FBW)	. E-plane Inline (0˚) . tapered ridge transition structure . small, low profile . Ridge WG structure . Fabrication errors are high . the loss tangent of this substrate is not well known in the terahertz band	. For measurements or system integrations in the terahertz band

VI. CONCLUSIONS

This review article provides an overview of various hybrid transition types. The author has proposed the most widely used microstrip to rectangular waveguide transitions for defence and satellites. All transitions have been covered in this work, which enables users to find the research gap, create their objectives, and also find some novel transition geometry. The study's design steps and mathematical expressions are interesting to use. In short, a complete method of generating RLC equivalent circuits from the S-parameters and resonance frequencies has been described. The article describes the detailed comparative study and review of the microstrip-to-waveguide transitions as per microwave bands from 4 GHz to 325 GHz. The article covers MS line-to-WG transitions in the microwave bands from the C-band (4 GHz–8 GHz) to the sub-mm wave band (220 GHz–325 GHz). The article also provides knowledge of dispersion parameters, i.e., the propagation constant. These help to evaluate the group velocity and phase velocities of dominant modes as well as higher-order modes. All confusing and similar definitions of the performance parameters of the microwave transitions have been defined more easily. A separate band-wise review has been illustrated in tabular form in terms of their performance parameter, a suitable substrate for the designated band, waveguide needed, coupling methodology used, mathematical expressions involved, their features based on merits and demerits, and their applications for microwave, mm-wave, sub-mm-wave, microwave imaging, automotive RADAR, satellite communications, MMIC, and planar circuits as interconnects for transmitters and receivers, power dividers, combiners, detectors, etc.

ACKNOWLEDGEMENT

The authors are grateful to the Hon'ble Vice-Chancellor, Gurukula Kangri (Deemed to be University), Haridwar, India for providing software and hardware support for conducting the project.

REFERENCES

[1] S. E. Hassan, M. Berggren, B. Scheiner, F. Michler, R. Weigel and F. Lurz, "Design of Planar Microstrip-to-Waveguide Transitions Using Topology Optimization", *IEEE Radio and Wireless Symposium (RWS)*, Orlando, Florida, USA, 16 May 2019, pp. 1-3, DOI: 10.1109/RWS.2019.8714566

[2] Y. Ren, K. Li, F. Wang, B. Gao and H. Wu, "A Broadband Magnetic Coupling Microstrip to Waveguide Transition Using Complementary Split Ring Resonators", in *IEEE Access*, vol. 7, pp. 17347-17353, 2019, DOI:10.1109/ACCESS.2019.2895159

[3] J. Li, J. Xu and J. Fu, "A Full Ka-Band Microstrip-to-Waveguide Transition Using Side-Inserted Magnetic Coupling Semicircular Ring", *Proc. IEEE Wireless Microw. Technol. Conf. (WAMICON)*, Apr. 2012, pp. 1-6, DOI: 10.1109/WAMICON.2012.6208434

[4] X. Huang and K.-L. Wu, "A Broadband U-slot Coupled Microstrip-to-Waveguide Transition", in *IEEE Trans. Microwave Theory Tech*, vol. 60, no. 5, pp. 1210-1217, May 2012, DOI: 10.1109/TMTT.2012.2187677

[5] N. Kaneda, Y. Qian and T. Itoh, "A Broad-Band Microstrip-to-Waveguide Transition Using Quasi-YagiAntenna", in *IEEE Trans. Microwave Theory Tech*, vol. 47, no. 12, pp. 2562-2567, Dec. 1999, DOI: 10.1109/22.809007

[6] Y. C. Shih, T. N. Ton and L. Q. Bui, "Waveguide-to-Microstrip Transitions for mm-Wave Applications", *IEEE MTT-S Int. Symp. Dig.*, vol. 1, New York, 1988, pp. 473-475, DOI: 10.1109/MWSYM.1988.22077

[7] W. Grapher, B. Hudler and W. Menzel, "Microstrip to Waveguide Transition Compatible with MM-wave Integrated Circuits", in *IEEE Trans. Microwave Theory Tech.*, vol. 42, pp. 1842-1843, September 1994, DOI: 10.1109/22.310597

[8] W. Grabherr and W. Menzel, "A New Transition from Microstrip Line to Rectangular Wave-Guide", *22nd European Microwave Conference*, 1992, Helsinki, Finland, pp. 1170-1175, DOI: 10.1109/EUMA.1992.335862

[9] F. J. Villegas, D. I. Stones and H. A. Hung, "A Novel Waveguide-to-Microstrip Transition for Millimeter-Wave Module Applications", in *IEEE Trans. Microwave Theory Tech.*, vol. 47, pp. 48-55, January 1999, DOI: 10.1109/22.740075

[10] D. Deslandes and K. Wu, "Integrated Microstrip and Rectangular Waveguide in Planar Form", in *IEEE Microwave and Wireless Components Letters*, vol. 11, no. 2, February 2001, DOI: 10.1109/7260.914305

[11] J. M. Pérez-Escudero, A. E. Torres-García, R. Gonzalo, and I. Ederra, "A Gap Waveguide-Based Compact Rectangular Waveguide to a Packaged Microstrip Inline Transition", in *Applied Sciences*, vol. 10, no. 14, Article 4979, Sep. 2020, DOI: 10.3390/app10144979

[12] S. Tomar, S. K. Singh, L. Suthar, R. B. Singh and A. Kumar, "E-Plane Waveguide to Microstrip Transition for Wave Applications", *ICMARS 2010*, December 2010

[13] J. H. C. Van Heuven, "A New Integrated Waveguide-Microstrip Transition", in *IEEE Transactions on Microwave Theory and Techniques*, March 1976, DOI: 10.1109/EUMA.1974.332108

[14] Z. Y. Malik, M. I. Nawaz and M. Kashif, "MMIC/MIC Compatible Planar Microstrip to Waveguide Transition at Ku-band for Radar Applications", *International Bhurban Conference on Applied Sciences & Technology*, Islamabad, Pakistan, 11-14 January 2010, pp. 51-53

[15] K. Sakakibara, M. Hirono, N. Kikuma and H. Hirayama, "Broadband and Planar Microstrip-to-Waveguide Transitions in mm-wave Band", *International Conference on Microwave and Wave Technology 2008*, Nanjing, China, DOI: 10.1109/icmmt.2008.4540667

[16] B. D. Nguyen, C. Migliaccio, Ch. Pichot and N. Rolland, "Design of Microstrip to Waveguide Transition in the W-Band Suitable Antenna or Integrated Circuits Connections", in *Microwave and Optical Technology Letters*, vol. 47, no. 6, December 20, 2005, pp. 518-520, DOI: 10.1002/mop.21216

[17] E. R. Murphy, *Microstrip to Waveguide Transition*, U.S. Patent, 4453142, June 1984

[18] T.-H. Lin and R.-B. Wu, "A Broadband Microstrip-to-Waveguide Transition with Tapered CPS Probe", *2002 32nd European Microwave Conference*, Milan, Italy, September, 2002, DOI: 10.1109/EUMA.002.339360

[19] H. Ijuka, T. Watanabe, K. Sato and K. Nishikawa, "Millimeter-Wave Microstrip Line to Waveguide Transition Fabricated on a Single Layer Dielectric Substrate", *R&D Review of Toyota*, CRDL, vol. 37, no. 2, Research report received on 23, April 2002

[20] Y. Lou, C. H. Chan and Q. Xue, "An In-line Waveguide-to-Microstrip Transition Using Radial-Shaped Probe", in *IEEE Microwave and Wireless Components Letters*, vol. 18, no. 5, May 2008, pp. 311-313, DOI: 10.1109/LMWC.2008.922114

[21] H. Aliakbarian, A. Enayati, G. A.E. Vandenbosch and W. De Raedt, "Novel Low-Cost End-Wall Microstrip-To-Waveguide Splitter Transition", in *Progress in Electromagnetics Research*, 2010, vol. 101, pp. 75-96, DOI:10.2528/pier 09081805

[22] R. Shireen, S. Shi and D. W. Prather, "W-band Microstrip-to-Waveguide Transition Using via Fences", in *Progress in Electromagnetics Research Letters*, vol. 16, pp. 151-160, August 2010, DOI: 10.2528/PIERL10061407

[23] C. Tang, X. Pan, F. Cheng and X. Lin, "A Broadband Microstrip-to-Waveguide End-wall Probe Transition and its Application in Waveguide Termination", in *Progress in Electromagnetics Research Letters*, January 2020, vol. 89, pp. 99-104, DOI: 10.2528/pierl19110601

[24] Z. Tong and A. Stelzer, "A Vertical Transition Between Rectangular Waveguide and Coupled Microstrip Lines", in *IEEE Microwave and Wireless Components Letters*, vol. 22, no. 5, May 2012, pp. 251-253, DOI: 10.1109/LMWC.2012.2192719

[25] A. K. Varshney, "A Microwave Rectangular Waveguide-to-Micro-strip line Transitions @ 30 GHz", in *International Journal of Emerging Technology and Advanced Engineering*, vol. 3, no. 8, August 2013.

[26] R.-Y. Fang and C.-L. Wang, "Miniaturized Microstrip-to-Waveguide Transition using Capacitance-Compensated Broadside-Coupled Microstrip Line", in *IEEE Transactions on Components, Packaging, and Manufacturing Technology*, vol. 3, no. 9, September 2013, DOI: 10.1109/TCPMT.2013.2244644

[27] A. Ariffin, D. Isa and A. Malekmohammadi, "Broadband Transition from Microstrip Line to Waveguide using a Radial Probe and Extended GND Planes for Millimeter-Wave Applications", in *Progress in Electromagnetics Research Letters*, vol. 60, pp. 95-100, May 26, 2016, DOI: 10.2528/PIERL16040801

[28] J. M. Pérez, A. Rebollo, R. Gonzalo and I. Ederra, "An Inline Microstrip-to-waveguide Transition Operating in the full W-Band based on a Chebyshev Multisection Transformer", *2016 10th European Conference on Antennas and Propagation (EuCAP)*, Davos, pp. 1-4, April 2016, DOI: 10.1109/ EuCAP.2016.7481796

[29] A. Ariffin and D. Isa, "Bandwidth Enhancement of Microstripline-to-Waveguide Transitions for Broadband E-band Module Applications", in *Microwave and Optical Technology Letters*, vol. 58, no. 6, June 2016, pp. 1398-1401, DOI: 10.1002/mop.29836

[30] J. M. Pérez-Escudero, A. E. Torres-García, R. Gonzalo and I. Ederra, "A Simplified Design Inline Microstrip-to-Waveguide Transition", in *Electronics*, 2018, vol. 7, no. 10, Article 215, DOI: 10.3390/electronics7100215

[31] M. Simone, A. Fanti, G. Valente, G. Montisci, R. Ghiani, and G. Mazzarella, "A Compact In-line Waveguide-to-Microstrip Transition in the Q-Band for Radio Astronomy Applications", in *Electronics*, February 2018, vol. 7, no. 2, Article 24, DOI: 10.3390/electronics7020024

[32] C. L. Li, C. Jin, H. Q. Ma and X. W. Shi, "An Inline Waveguide-to-Microstrip Transition for Wideband Millimeter-Wave Applications", in *Microwave and Optical Technology Letters*, pp. 1-5, December 2019, DOI: 10.1002/mop.32199

[33] Z. Liu, J. Xu and W. Wang, "Wideband Transition from Microstrip Line-to-Empty Substrate-Integrated Waveguide Without Sharp Dielectric Taper", in *IEEE Microwave and Wireless Components Letters*, vol. 29, no. 1, pp. 20-22, January 2019, DOI: 10.1109/LMWC.2018.2881055

[34] P. Hügler, T. Chaloun and C. Waldschmidt, "A Wideband Differential Microstrip-to-Waveguide Transition for Multilayer PCBs at 120 GHz", in *IEEE Microwave and Wireless Components Letters*, vol. 30, no. 2, pp. 170-172, February 2020, DOI: 10.1109/LMWC.2019.2958208

[35] A. Meyer, S. Karau and M. Schneider, "Broadband Stacked-Patch Transition from Microstrip Line to Circular Dielectric Waveguide for Dual-Polarized Applications at W-Band Frequencies", *2019 49th European Microwave Conference (EuMC)*, Paris, France, 2020, pp. 440-443, DOI: 10.23919/EuMC.2019.8910938

[36] D. M. Pozar, *Microwave Engineering*, Wiley Student Edition, 4th edition, pp. 148-149, reprints 2016, ISBN 978-0-470-63155-3

[37] S. Y. Liao, *Microwave Devices and Circuits*, Pearson Prentice Hall, 3rd edition, 2007

[38] R. Gupta and P. P. Kumar, "Improved Design of Ka-band Waveguide to Coaxial Right Angle Microwave Transition", *URSI RCRS 2020*, IIT (BHU), Varanasi, India, 12-14 February 2020, DOI: 10.23919/URSIRCRS49211.2020.9113526

[39] Y. Tahara, A. Ohno, H. Oh-hashi, S. Makino, M. Ono and T. Ohba, "A Novel Microstrip-to-Waveguide Transition Using Electromagnetic Band Gap Structure", *Proceedings of ISAP*, Seoul, Korea, 2005, pp. 459-462. DOI:10.34385/proc.33.2D1-2

[40] K.-Y. Li and Y.-H. Cheng, "An Inline Microstrip-to-Waveguide Transition at 300 GHz", *2021 IEEE International Symposium on Radio-Frequency Integration Technology (RFIT)*, 2021, pp. 1-2. DOI: 10.1109/RFIT52905.2021.9565230

[41] M. Somanath, C. Saha, H. Tolani and P. Chakraborty, "A Novel G-Band E-plane Waveguide to Microstrip Transition for Sub-Millimeter-Wave/THz Application", *2020 IEEE International Symposium on Antennas and Propagation and North American Radio Science Meeting*, Montreal, QC, Canada, 2020, pp. 1605-1606, DOI:10.1109/IEEECONF35879.2020.9329675

[42] O. Donadio, K. Elgaid and R. Appleby, "Waveguide to Microstrip at G Band Using Elevated E Plane Probe", in *Electronics Letters*, vol. 47, iss. 2, pp. 115-116, Jan. 2011, DOI: 10.1049/el.2010.2926

[43] E. Daniel, V. Sokolov, S. Sommerfeldt, J. Bublitz, K. Olson and B. Gilbert, "Packaging of Microwave Integrated Circuits Operating Beyond 100 GHz", *Proceedings. IEEE Lester Eastman Conference on High-Performance Devices*, Newark, DE, USA, Aug. 2002, pp. 374-383, DOI: 10.1109/LECHPD.2002.1146777

[44] A. Tessmann, A. Leuther, M. Kuri, H. Massler, M. Riessle, H. Essen, S. Stanko, R. Sommer, M. Zink, R. Stibal, W. Reinert and M. Schlechtweg, "220GHz Low-Noise Amplifier Modules for Radiometric Imaging Applications", *2006 European Microwave Integrated Circuits Conference*, Manchester, UK Sep. 2006, pp. 137 –140. DOI: 10.1109/EMICC.2006.282770

[45] H. Aliakbarian, S. Radiom, Guy A. E. Vandenbosch and G. Gielen. "A Fully Micromachined Double Slot Waveguide to GCPW Transition for 180-230 GHz mm-Wave Application", *2014 IEEE International Conference on Ultra-WideBand (ICUWB*), Phoenix, AZ, USA, May 2015, pp. 394-397, DOI: 10.1109/ICUWB.2014.6959014

[46] S. Kumari and P. Mondal, "Full U-Band Rectangular Waveguide-to-Microstrip Transition Using E-Plane Probe", *11th International Radar Symposium India – 2017, (IRSI-17)*, Nimhans Convention Centre, Bangalore INDIA, 2017, pp. 1-4.

[47] A. Hassona, Z. S. He, O. Habibpour, V. Desmaris, V. Vassilev and S. Yang, "A Low-Loss D-Band Chip-to-Waveguide Transition Using the Unilateral Fin-Line Structure", *2018 IEEE/MTT-S Int. Microw Symp*, Philadelphia, PA, USA, 2018, pp. 390-393, DOI: 10.1109/MWSYM.2018.8439643

[48] A. Hassona, V. Vassilev, Z. S. He, A. Zaman, C. Mariotti, F. Dielacher and H. Zirath, "D-Band Waveguide-to-Microstrip Transition Implemented in eWLB Packaging

Technology", in *Electronics Letters*, vol. 56, no. 4, 2020, pp. 187–189, DOI: 10.1049/el.2019.3331

[49] W. Xu, F. Liu and H. Xu., "A Novel Ultra-Wideband Waveguide-to-Microstrip Transition for Millimeter-Wave Applications", in *AIP Advances 6*, vol. 6, no. 2, 2016, pp. 105001-1-105001-5, DOI: 105001-1-105001-7

[50] A. Hassona, Z. S. He, C. Mariotti, F. Dielacher, V. Vassilev and Y. Li "A Non-Galvanic D-Band MMIC-to-Waveguide Transition Using eWLB Packaging Technology", *2017 IEEE MTT-S Int. Microwave Symp*., Honololu, HI, USA, 2017, pp. 510–512, DOI: 10.1109/MWSYM.2017.8058612

[51] A. Hassona, V. Vassilev, Z. S. He, C. Mariotti, F. Dielacher and H. Zirath, "Silicon Taper-Based D-Band Chip to Waveguide Interconnect for Millimeter-Wave Systems", in *IEEE Microw. Wirel. Compon. Lett.*, vol. 27, iss. 12, 2017 pp. 1092–1094, DOI: 10.1109/LMWC.2017.2763118

[52] Y.-C. Leong and S. Weinreb, "Full Band Waveguide-to-Microstrip Probe Transitions", *1999 IEEE MTT-S International Microwave Symposium Digest*, vol. 4, Anaheim, CA, USA, 1999, pp. 1435–1438, DOI:10.1109/MWSYM.1999.780219

[53] A. Varshney and V. Sharma, "A Comparative Study of Microwave Rectangular Waveguide-to-Microstrip Line Transition for Millimeter-wave, Wireless Communications and Radar Applications", in *Microwave Review*, vol. 2, no. 26, Dec. 2020, pp. 26-37, ISSN 14505835

[54] W. Maeda, K. Sakakibara N. Kikuma and H. Hirayama, "Design of Millimeter-Wave Detector Module Composed of Detector Circuit and Waveguide-to-Microstrip Transition", *2009 International Symposium on Antennas and Propagation (ISAP 2009)*, Bangkok, Thailand, Oct. 20-23, 2009, pp. 369-372

[55] T. S. Bird, "Definition and Misuse of Return Loss [Report of the Transactions Editor-in-Chief]", in *IEEE Antennas and Propagation Magazine*, vol. 51, no. 2, April 2009, pp. 166–167, DOI: 10.1109/MAP. 2009.5162049

[56] A. Varshney, V. Sharma, I. Elfergani, C. Zebiri, Z. Vujicic and J. Rodriguez, "An Inline V-Band WR-15 Transition Using Antipodal Dipole Antenna as RF Energy Launcher @ 60 GHz for Satellite Applications", in *Electronics*, vol. 11, 2022, 3860, pp. 1-16, DOI: 10.3390/electronics11233860

[57] A. Varshney, V. Sharma and R. Kumar, "Microstrip Interconnect Design and Modeling Using Reverse Approach to Obtain an Efficient Wideband MS Line-to-RWG Hybrid Transition", *Printed antennas: Design and Challenges*, book chapter 5, Tylor and Francis, CRC Press, Ch 05, 2022, pp. 67-80, DOI: 10.1201/9781003347057-5

[58] A. Varshney and V. Sharma, "An Economic Low-profile MSL-to-RWG Transition using Microstrip Antenna as Launcher for X-Band Applications", in *IJEER*, Forex Publication, vol. 10, no. 2, 2022, pp. 1-7

[59] A. Varshney, V. Sharma, C. Nayak, A. K. Goyal and Y. Massoud, "A Low-Loss Impedance Transformer-Less Fish-Tail-Shaped MS-to-WG Transition for K-/Ka-/Q-/U-Band Applications", in *Electronics*, vol. 12, p. 670, 2023, DOI: 10.3390/electronics12030670

[60] A. Varshney, V. Sharma and A. Agarwal, "A W-Band Metallic Via-Based Inline Microstrip-to-WR10 Transition for mm-Wave, Satellite, and Radar Applications", in *Journal of The Institution of Engineers (India)*, Series B, pp. 1-10, 2023, DOI: 10.1007/s40031-023-00944-6

[61] A. Varshney, V. Sharma, A. Agarwal, "Next-Generation MS-to-RWG Interconnects for Microwave and mm-Wave Communications Using Microstrip Antenna as RF Energy Launcher @ 140 GHz", in *Journal of The Institution of Engineers (India)*, Series B pp. 1-6, 2023, DOI: 10.1007/s40031-023-00944-6

[62] A. Varshney and V. Sharma, "Aerodynamic Slotted SIW-to-MS Line Transition Using Mitered End Taper for Satellite and Radar Communications", in *World Journal of Engineering*, © Emerald Publishing Limited, vol. 21, iss. 3, 2024, pp. 588-603, DOI: 10.1108/WJE-08-2022-0330

[63] K. Chang, *RF and Microwave Wireless Systems*, Wiley, reprints 2015, pp. 90-97, ISBN 10: 8126556218

[64] A. Varshney and V. Sharma, "A Comparative Study of Conventional Transition Model and Reverse Transition Model for Wireless and Radar Applications", in *SAMRIDDHI: A Journal of Physical Sciences, Engineering and Technology*, vol. 15, no. 3, 2023, pp. 346-353, DOI: 10.18090/samriddhi.v15i03.11